

Effect of Co doping and hydrostatic pressure on SrFe_2As_2

E. Lengyel¹, M. Kumar^{1,†}, W. Schnelle¹, A. Leithe-Jasper¹, and M. Nicklas^{1,*}

¹ Max Planck Institute for Chemical Physics of Solids, Nöthnitzer Str. 40, 01187 Dresden, Germany.

Key words: superconductivity, iron-based superconductors, pressure experiments.

* Corresponding author: e-mail nicklas@cpfs.mpg.de

† Present address: Malaviya National Institute of Technology Jaipur, Department of Physics, Jaipur 302017, Rajasthan, India.

We report a pressure study on electron doped $\text{SrFe}_{2-x}\text{Co}_x\text{As}_2$ by electrical-resistivity (ρ) and magnetic-susceptibility (χ) experiments. Application of either external pressure or Co substitution rapidly suppresses the spin-density wave ordering of the Fe moments and induces superconductivity in SrFe_2As_2 . At $x = 0.2$ the broad superconducting (SC) dome in the $T - p$ phase diagram exhibits its maximum $T_{c,\text{max}} = 20$ K at a pressure of only $p_{\text{max}} \approx 0.75$ GPa. In $\text{SrFe}_{1.5}\text{Co}_{0.5}\text{As}_2$ no superconductivity is observed anymore up to 2.8 GPa.

Upon increasing the Co concentration the maximum of the SC dome shifts toward lower pressure accompanied by a decrease in the value of $T_{c,\text{max}}$. Even though, superconductivity is induced by both tuning methods, Co substitution leads to a much more robust SC state. Our study evidences that in $\text{SrFe}_{2-x}\text{Co}_x\text{As}_2$ both, the effect of pressure and Co-substitution, have to be considered in order to understand the SC phase-diagram and further attests the close relationship of SrFe_2As_2 and its sister compound BaFe_2As_2 .

Copyright line will be provided by the publisher

1 Introduction The parent compounds AFe_2As_2 ($\text{A}=\text{Ca}, \text{Sr}, \text{Ba}, \text{Eu}$) of the iron-pnictide superconductors exhibit at ambient pressure a spin-density wave (SDW) instability at T_{SDW} which is associated with a tetragonal to orthorhombic structural phase transition [1,2]. Doping with K, Cs, or Na at the A site (hole doping) [3,4,5,6,7] or partial replacement of Fe with Co or Ni (electron doping) [7,8,9,10] suppresses the SDW transition rapidly. Alternatively T_{SDW} can be suppressed by application of external pressure [11,12,13]. In both cases, superconductivity starts to develop in the region where T_{SDW} becomes zero. In SrFe_2As_2 , for example, superconductivity has been confirmed on doping with K, Cs, or Na at the Sr-site (hole doping) [3,4,5,6,7] or partial replacement of Fe by Co or Ni (electron doping) [7,8,9] as well as under external pressure [11,12,14,15,16,17,18,19,20,21,22].

While pressure-induced superconductivity in stoichiometric SrFe_2As_2 [11,12,14,15,16,17,18,19,20,21,22] as well as superconductivity on electron- and hole-doping has been studied extensively [4,5,6,7,8,9,23,24,25,26], only one combined pressure – hole-doping study has been reported in $\text{Sr}_{1-x}\text{K}_x\text{Fe}_2\text{As}_2$ [27], but no pressure – electron-doping investigation. Substituting Fe by Co in

$\text{SrFe}_{2-x}\text{Co}_x\text{As}_2$ corresponds to an electron doping directly inside the iron-arsenide layers. Upon increasing the Co concentration the SDW transition is suppressed rapidly from $T_{\text{SDW}} = 205$ K in undoped SrFe_2As_2 to 95 K at a Co concentration of $x = 0.15$ [8]. At $x = 0.2$ no indication of the SDW anomaly is observed neither in resistivity nor in magnetic-susceptibility experiments [8]. Superconductivity develops in the concentration range $0.2 \leq x \leq 0.4$. The bulk nature of the superconductivity has been confirmed by specific-heat measurements [8]. The maximum T_c of $T_{c,\text{max}} = 19.4$ K is already observed at $x = 0.2$, which is the lowest Co concentration where superconductivity appears. With further increasing Co concentration T_c decreases monotonically. Finally, $\text{SrFe}_{1.5}\text{Co}_{0.5}\text{As}_2$ is not superconducting (SC) anymore. The $T - x$ phase diagram of $\text{SrFe}_{2-x}\text{Co}_x\text{As}_2$ resembles that of the temperature – pressure ($T - p$) phase diagram of stoichiometric SrFe_2As_2 . Here, on application of hydrostatic pressure T_{SDW} is suppressed between 3 and 4 GPa [11]. In this pressure range also superconductivity appears [11]. The bulk nature of the SC phase has been confirmed by magnetization and susceptibility data [14]. However, there is a discrepancy in literature on the actual pressure range

Copyright line will be provided by the publisher

where superconductivity is observed [11, 12, 14, 15, 16, 17, 18, 19, 20, 21, 22].

In this paper we compare the effect of electron doping inside the iron-arsenide layers by substituting Fe by Co and the application of hydrostatic pressure on the SDW transition as well as on the SC properties of SrFe_2As_2 . While there is no data available on the combined effect of Co-substitution and pressure in SrFe_2As_2 , its stoichiometric sister compound BaFe_2As_2 has been studied in details [28, 29, 30, 31, 32, 33, 34]. In order to establish the $T - p$ phase diagram of $\text{SrFe}_{2-x}\text{Co}_x\text{As}_2$ and to compare it with the findings in $\text{BaFe}_{2-x}\text{Co}_x\text{As}_2$, we carried out electrical-resistivity experiments under hydrostatic pressure on three different $\text{SrFe}_{2-x}\text{Co}_x\text{As}_2$ samples with the concentrations $x = 0.1, 0.2$, and 0.5 . The samples were chosen in a way to be in the underdoped ($x = 0.1$, SDW and no superconductivity), optimally doped ($x = 0.2$, no SDW and superconductivity), and overdoped ($x = 0.5$, no SDW and no superconductivity) at atmospheric pressure regime. We will demonstrate that the application of pressure gradually suppresses T_{SDW} and induces superconductivity in $\text{SrFe}_{1.9}\text{Co}_{0.1}\text{As}_2$, but at much lower pressures and with a much smaller $T_{c,\text{max}}$ compared with stoichiometric SrFe_2As_2 . For $x = 0.2$ superconductivity appears in a dome-like shape in an extended pressure range. No superconductivity is induced in $\text{SrFe}_{1.5}\text{Co}_{0.5}\text{As}_2$. The electrical-resistivity studies are complemented by magnetic-susceptibility investigations on $\text{SrFe}_{1.85}\text{Co}_{0.15}\text{As}_2$ under pressure.

2 Methods Polycrystalline samples were synthesized by sintering stoichiometric amounts of the precursors SrAs, Fe_2As and Co_2As (for details see Ref. [8]). X-ray diffraction measurements confirmed the ThCr_2Si_2 -type structure (space group $I4/mmm$) for all samples [8]. Temperatures down to 1.8 K and magnetic fields up to 14 T were generated using a cryostat equipped with a superconducting magnet (PPMS, Quantum Design). In a double-layer piston-cylinder type cell pressures up to 2.8 GPa have been achieved with silicon oil as pressure transmitting medium [35]. A piece of lead was used as manometer. Measurements of the electrical resistivity were carried out using a standard four-probe technique utilizing a LR700 (Linear Research) resistance bridge. The magnetic field was applied perpendicular to the electrical current. Magnetic-susceptibility measurements were conducted with a miniaturized coil system consisting of one primary coil and one pair of compensated secondary coils sitting inside the pressure cell. Here the LR700 served as mutual-inductance bridge. A frequency of $\nu = 16$ Hz and a modulation field, H_{AC} , in the range between 0.06 and 20 Oe were used. The sample was placed in the center of one of the secondary coils. In order to obtain absolute values of the sample susceptibility we used the size of the diamagnetic signal of the piece of lead sitting next to

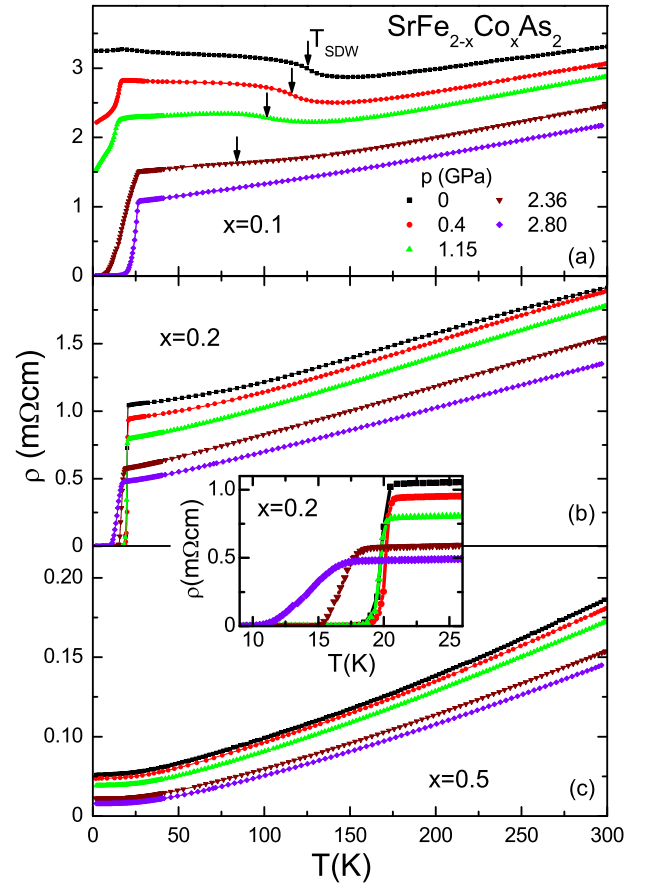


Figure 1 Electrical resistivity of $\text{SrFe}_{2-x}\text{Co}_x\text{As}_2$ ($x = 0.1, 0.2$, and 0.5) for selected pressures. T_{SDW} is marked by arrows [36]. Inset: low-temperature electrical resistivity of $\text{SrFe}_{1.8}\text{Co}_{0.2}\text{As}_2$.

the sample and set it to -1 . This procedure allowed us to estimate the SC volume fraction of our sample.

3 Results and discussion Figure 1 displays the electrical resistivity $\rho(T)$ of $\text{SrFe}_{2-x}\text{Co}_x\text{As}_2$ ($x = 0.1, 0.2$, and 0.5) for selected pressures. At all investigated pressures, $\rho(T)$ decreases monotonically upon decreasing temperature indicating metallic behavior. Only for $x = 0.1$ a pronounced upturn in $\rho(T)$ toward lower temperatures indicates the SDW transition of the itinerant iron moments, which is associated with a structural transition from a tetragonal to an orthorhombic phase. The increase in $\rho(T)$ at T_{SDW} [36], is distinct from the sharp drop observed in undoped SrFe_2As_2 [2], but is in good agreement with reports on other doped AFe_2As_2 compounds [8, 28, 37, 38]. The different behavior in the electrical resistivity at T_{SDW} might be related to disorder introduced by the Co substitution. In $\text{SrFe}_{1.9}\text{Co}_{0.1}\text{As}_2$ application of pressure shifts the anomaly at the SDW transition from $T_{\text{SDW}} = 125$ K at ambient pressure to 72 K at 2.60 GPa. The anomaly

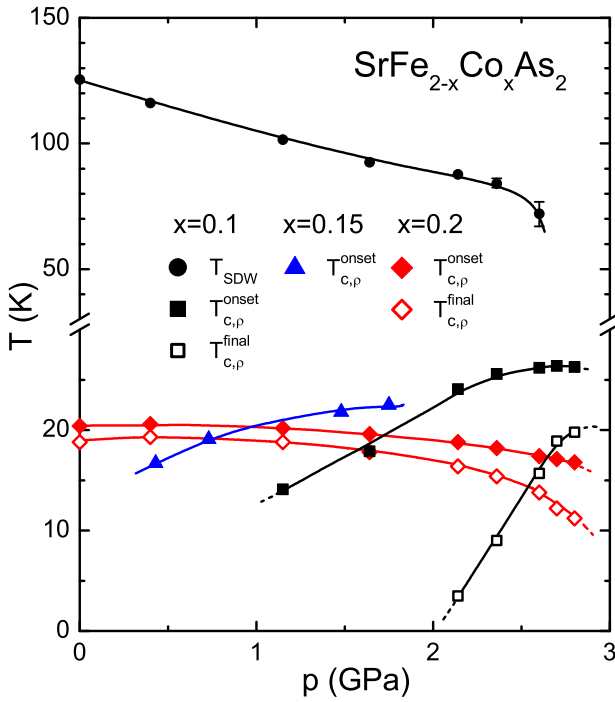


Figure 2 $T - p$ phase diagram of $\text{SrFe}_{2-x}\text{Co}_x\text{As}_2$, $x = 0.1, 0.15$ (resistivity data not shown), and 0.2 . T_{SDW} , $T_{c,p}^{\text{onset}}$, and $T_{c,p}^{\text{final}}$ obtained from the electrical resistivity as function of pressure [39].

in $\rho(T)$ broadens and becomes less pronounced with increasing pressure. At 2.8 GPa we do not find any feature related to the SDW transition in our data anymore suggesting that $T_{\text{SDW}}(p)$ is suppressed to zero at a critical pressure p_c between 2.6 and 2.8 GPa. The resistivity curves of $\text{SrFe}_{2-x}\text{Co}_x\text{As}_2$, $x = 0.2$ and 0.5 , do not show any qualitative change in shape upon increasing pressure (see Fig. 1). While $\text{SrFe}_{1.9}\text{Co}_{0.1}\text{As}_2$ and $\text{SrFe}_{1.8}\text{Co}_{0.2}\text{As}_2$ become superconducting, $\text{SrFe}_{1.5}\text{Co}_{0.5}\text{As}_2$ does not show any indication of the formation of a SC state in the whole investigated pressure range up to 2.8 GPa.

In $\text{SrFe}_{1.9}\text{Co}_{0.1}\text{As}_2$ a small reduction in $\rho(T)$ below 15 K indicates the presence of some spurious superconductivity already at ambient pressure (see Fig. 1a), which might be induced by internal strains [9]. Upon increasing pressure the drop in $\rho(T)$ becomes more pronounced and its onset shifts to higher temperatures. Finally, at $p = 2.36$ GPa a zero-resistance state is observed below $T_{c,p}^{\text{final}} = 4.0$ K [39]. We note that at this pressure the SDW transition is still present at $T_{\text{SDW}} = 84$ K along with superconductivity at low temperatures. The step in $\rho(T)$ becomes sharper and $T_{c,p}^{\text{final}}$ increases up to 19.8 K at 2.8 GPa. The increase in T_c coincides with a considerable narrowing of the transition anomaly in the resistivity, as shown in the $T - p$ phase diagram in Fig. 2. The width of the SC transition decreases upon increasing pressure from $\Delta T_c = T_{c,p}^{\text{onset}} -$

$T_{c,p}^{\text{final}} = 20.6$ K at 2.14 GPa to only 6.5 K at 2.8 GPa. While $T_{c,p}^{\text{final}}$ still increases slightly up to our highest pressure $p = 2.8$ GPa, $T_{c,p}^{\text{onset}}$ achieves its maximum already at 2.7 GPa denoting that the maximum of the SC dome is almost reached. This indicates that in $\text{SrFe}_{1.9}\text{Co}_{0.1}\text{As}_2$ $T_{c,\text{max}}$ is smaller than in the undoped mother compound [?]. One reason might be the disorder induced in the iron-arsenide layers by the Co substitution which could limit T_c under pressure.

We now turn to $\text{SrFe}_{1.8}\text{Co}_{0.2}\text{As}_2$, where at ambient pressure no SDW order is present anymore. A drop in $\rho(T)$ to zero at $T_{c,p}^{\text{final}} = 18.8$ K indicates the existence of superconductivity already at atmospheric pressure. The bulk nature of the SC phase has been confirmed by magnetic-susceptibility and specific-heat experiments [8]. The effect of pressure on T_c is initially rather weak. The inset of Fig. 1 displays a magnification of the resistivity in the low-temperature region. Upon application of pressure the SC transition temperature first increases slightly up to $T_{c,\text{max}} = 19.3$ K at 0.4 GPa before it starts to decrease again, indicating that $\text{SrFe}_{1.8}\text{Co}_{0.2}\text{As}_2$ is still situated on the left side of the SC dome, in the under-doped regime, in the $T - x$ phase diagram. Above 1.5 GPa, $T_{c,p}^{\text{final}}(p)$ starts to drop faster upon increasing pressure as depicted in Fig. 2. In the region of the maximum of the SC dome we observe a rather narrow SC transition, $\Delta T_c = 1.3$ K. This value is considerably smaller than in the case of $\text{SrFe}_{1.9}\text{Co}_{0.1}\text{As}_2$ despite the higher Co concentration. This might indicate that disorder induced by Co substitution has only a minor effect on the width of the SC transition. With increasing distance to $T_{c,\text{max}}$ ΔT_c increases slightly, but still remains much smaller than in $\text{SrFe}_{1.9}\text{Co}_{0.1}\text{As}_2$.

The effect of pressure on SrFe_2As_2 resembles that of Co-substitution on the iron site [8, 11]. However, the maximum SC transition temperature is larger in pressurized compared with Co-doped SrFe_2As_2 . Our study shows that this is a general trend in the combined $T - p - x$ phase diagram of $\text{SrFe}_{2-x}\text{Co}_x\text{As}_2$: $T_{c,\text{max}}$ observed under pressure decreases and shifts toward lower temperatures upon increasing the Co concentration. At the same time superconductivity develops in an extended pressure interval. A similar behavior has been previously established for $\text{BaFe}_{2-x}\text{Co}_x\text{As}_2$ [28, 29, 30, 31, 32, 33, 34]. Thus our study provides additional experimental evidence for the close relation of the Sr- and Ba-variants of the 122 iron-pnictide superconductors.

In $\text{SrFe}_{1.9}\text{Co}_{0.1}\text{As}_2$ we have also investigated the effect of a magnetic field on the SC transition at 2.8 GPa close to the maximum of the SC dome. The results of the $\rho(T)$ experiments carried out in different magnetic fields up to 14 T are displayed in Fig. 3. We note that the transition slightly broadens upon increasing the magnetic field. This is expected in a polycrystalline material possessing an anisotropic $H_{c2}(T)$ as anticipated for a quasi-two dimensional electronic structure [26]. The $H_{c2}(T)$ curves obtained from $T_{c,p}^{\text{onset}}$, $T_{c,p}^{\text{mid}}$, and $T_{c,p}^{\text{final}}$ are displayed in

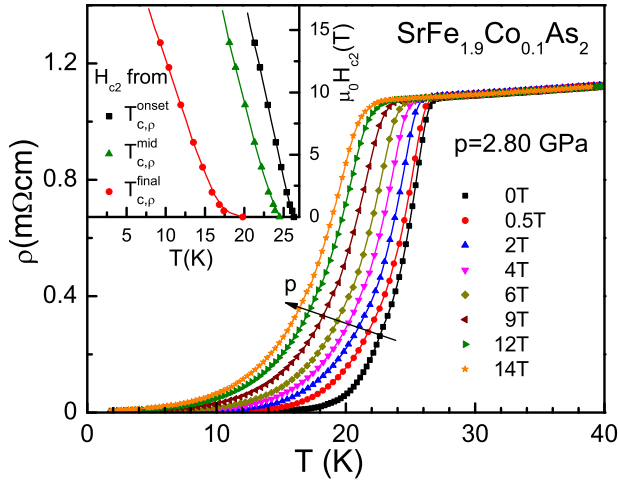


Figure 3 Electrical resistivity of SrFe_{1.9}Co_{0.1}As₂ at 2.8 GPa in different applied magnetic fields. Inset: $H_{c2} - T$ diagram for H_{c2} determined from $T_{c,\rho}^{\text{onset}}$, $T_{c,\rho}^{\text{mid}}$, and $T_{c,\rho}^{\text{final}}$ [39].

the inset of Fig. 3. A minor tail in $H_{c2}(T)$ is visible at small magnetic fields. It is most pronounced in the $H_{c2}^{\text{final}}(T)$ curve. It is likely to be related with multiband effects. Disregarding this tail, we obtain an initial slope of $\mu_0 dH_{c2}^{\text{final}}(T)/dT \approx -1.8$ T/K.

In addition to the electrical-resistivity studies, we carried out detailed magnetic-susceptibility measurements on SrFe_{1.85}Co_{0.15}As₂ under external pressure. Figure 4 depicts the temperature dependence of the real χ'_V and imaginary χ''_V parts of the volume susceptibility at different pressures. $\chi'_V(T)$ at 0.05 GPa already displays a small diamagnetic response of about 10% of the sample volume at 1.8 K. Upon increasing pressure the SC volume fraction rapidly increases. At 1.05 GPa $\chi'_V(T)$ tends to saturate toward the lowest temperatures at about -0.7 indicating a diamagnetic signal corresponding to 70 % of the sample volume. Within the accuracy of our experiment this value does not change up to $p = 2.58$ GPa, the highest pressure in our experiment. Considering the uncertainties in the estimation of the SC volume fraction, our results indicate that almost the complete sample becomes SC in the pressure range above 1.05 GPa.

The effect of a magnetic field on $\chi'_V(T)$ at 2.3 GPa, close to the maximum of the SC dome, is shown in Fig. 5. The SC volume fraction decreases fast upon increasing the magnetic field and does not saturate anymore down to the lowest temperatures already in the smallest applied field of 0.1 T. At 9 T we find a SC volume fraction of only 25% remaining.

At 2.3 GPa, $\chi'_V(T)$ exhibits a sharp drop at the onset of the diamagnetic response, but develops a shoulder at lower temperatures. This shoulder is also present at smaller pressures, but less prominent. This two-step SC transition is known for polycrystalline samples and is related to the

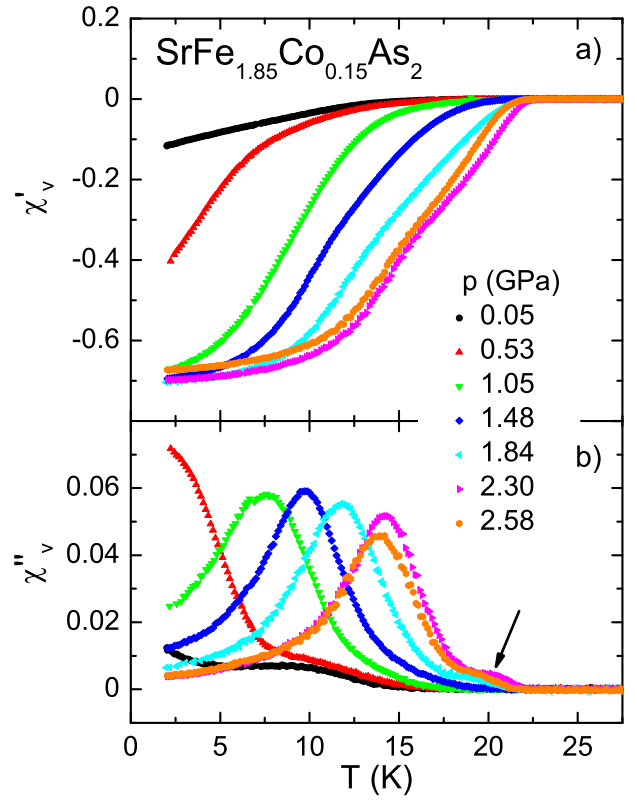


Figure 4 (a) Real and (b) imaginary parts of the volume susceptibility of SrFe_{1.85}Co_{0.15}As₂ at different pressures. The data were taken with an excitation frequency of 16 Hz and an amplitude of the oscillation field of 1.33 Oe. The arrow in (b) marks the shoulder in $\chi''_V(T)$ attributed to intra-grain superconductivity. See text for details.

granularity of the material. It has been investigated in details in the high-temperature cuprate superconductors [40]. Upon cooling first intra-grain superconductivity develops before inter-grain coherence is established at lower temperatures. $\chi'_V(T)$ displays a large peak related to loss due to the coupling between the grains, while only a small feature is visible at the onset of the diamagnetic response arising from flux entry into the grains (see Fig. 4). As expected, the amplitude of the oscillation field has a strong influence on inter-grain effects as visible in the magnetic susceptibility displayed in Fig. 6. Upon changing the amplitude from $H_{AC} = 0.0665$ to 19.95 Oe by a factor of 300, the onset of the diamagnetic signal is almost unaltered. There is only little influence on the initial drop in $\chi'_V(T)$, since this drop originates from the development of superconductivity in individual grains. However, we find large changes due to inter-grain effects in both, real and imaginary parts of the susceptibility: increasing H_{AC} reduces the diamagnetic signal and shifts the inter-grain loss peak strongly toward lower temperatures. At the same time a second peak

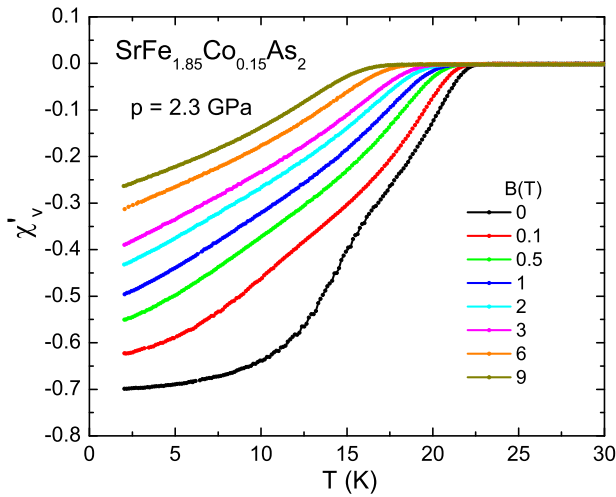


Figure 5 Real part of the volume susceptibility of $\text{SrFe}_{1.85}\text{Co}_{0.15}\text{As}_2$ at 2.3 GPa measured in different magnetic fields upon warming, after cooling the sample in zero magnetic field. The data were taken with an excitation frequency of 16 Hz and an amplitude of the oscillation field of 1.33 Oe.

(shoulder) at higher temperatures associated with the flux entry into the grains becomes more pronounced.

4 Summary We carried out a combined Co-substitution and hydrostatic-pressure study for SrFe_2As_2 materials, where substituting Fe by Co directly corresponds to electron doping into the iron-arsenide layers. Co substitution as well as application of pressure leads to a suppression of the SDW transition and the development of a SC phase in a similar way like in BaFe_2As_2 . We observe a SC dome in the $T-p$ phase diagram for $\text{SrFe}_{2-x}\text{Co}_x\text{As}_2$, $x = 0.1, 0.15$, and 0.2 . Its maximum shifts systematically toward lower pressures with increasing Co concentration. At the same time the maximum T_c decreases, but superconductivity extends to a larger pressure range in the $T-p$ phase diagram indicating a more robust SC state.

5 Acknowledgements We thank the Deutsche Forschungsgemeinschaft (DFG) for financial support through SPP 1458.

References

- [1] M. Rotter, M. Tegel, D. Johrendt, I. Schellenberg, W. Hermes, and R. Pöttgen, *Phys. Rev. B* **78**, 020503(R) (2008).
- [2] A. Jesche, N. Caroca-Canales, H. Rosner, H. Borrmann, A. Ormeci, D. Kasinathan, H. H. Klauss, H. Luetkens, R. Khasanov, A. Amato, A. Hoser, K. Kaneko, C. Krellner, and C. Geibel, *Phys. Rev. B* **78**, 180504(R) (2008).
- [3] M. Rotter, M. Tegel, and D. Johrendt, *Phys. Rev. Lett.* **101**, 107006 (2008).
- [4] K. Sasmal, B. Lu, B. Lorenz, A. M. Guloy, F. Chen, Y. Xue, and C. Chu, *Phys. Rev. Lett.* **101**, 107007 (2008).

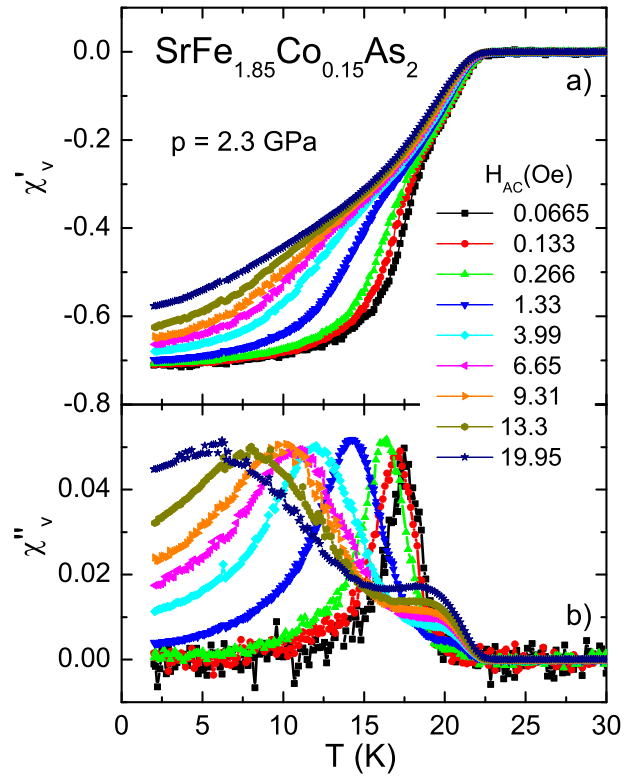


Figure 6 (a) Real and (b) imaginary parts of the volume susceptibility of $\text{SrFe}_{1.85}\text{Co}_{0.15}\text{As}_2$ at 2.3 GPa measured in zero magnetic field with different amplitudes of the oscillation field H_{AC} . The data were taken with an excitation frequency of 16 Hz.

- [5] G. F. Chen, Z. Li, G. Li, W. Z. Hu, J. Dong, X. D. Zhang, P. Zheng, N. L. Wang, and J. L. Luo, *Chin. Phys. Lett.* **25** 3403 (2008).
- [6] T. Goko, A. A. Aczel, E. Baggio-Saitovitch, S. L. Bud'ko, P. C. Canfield, J. P. Carlo, G. F. Chen, Pengcheng Dai, A. C. Hamann, W. Z. Hu, H. Kageyama, G. M. Luke, J. L. Luo, B. Nachumi, N. Ni, D. Reznik, D. R. Sanchez-Candela, A. T. Savici, K. J. Sikes, N. L. Wang, C. R. Wiebe, T. J. Williams, T. Yamamoto, W. Yu, and Y. J. Uemura, *Phys. Rev. B* **80**, 024508 (2009).
- [7] D. Kasinathan, A. Ormeci, K. Koch, U. Burkhardt, W. Schnelle, A. Leithe-Jasper, H. Rosner, *New J. Phys.* **11**, 025023 (2009).
- [8] A. Leithe-Jasper, W. Schnelle, C. Geibel, and H. Rosner, *Phys. Rev. Lett.* **101** 207004 (2008).
- [9] S. R. Saha, N. P. Butch, K. Kirshenbaum, and J. Paglione, *Phys. Rev. B* **79**, 224519 (2009).
- [10] A. S. Sefat, R. Jin, M. A. McGuire, B. C. Sales, D. J. Singh, and D. Mandrus, *Phys. Rev. Lett.* **101**, 117004 (2008).
- [11] M. Kumar, M. Nicklas, A. Jesche, N. Caroca-Canales, M. Schmitt, M. Hanfland, D. Kasinathan, U. Schwarz, H. Rosner, and C. Geibel, *Phys. Rev. B* **78**, 184516 (2008).
- [12] E. Colombier, S. L. Bud'ko, N. Ni, and P. C. Canfield, *Phys. Rev. B* **79**, 224518 (2009).

- [13] C. F. Miclea, M. Nicklas, H. S. Jeevan, D. Kasinathan, Z. Hossain, H. Rosner, P. Gegenwart, C. Geibel, and F. Steglich, *Phys. Rev. B* **79**, 212509 (2009).
- [14] P. L. Alireza, Y. T. C. Ko, J. Gillett, C. M. Petrone, J. M. Coole, G. G. Lonzarich and S. E. Sebastian, *J. Phys.: Condens. Matter* **21** 012208 (2008).
- [15] M. S. Torikachvili, S. L. Bud'ko, N. Ni, and P. C. Canfield, *Phys. Rev. B* **78**, 104527 (2008).
- [16] K. Matsubayashi, N. Katayama, K. Ohgushi, A. Yamada, K. Munakata, T. Matsumoto, and Y. Uwatoko, *J. Phys. Soc. Jpn.* **78**, 073706 (2009).
- [17] K. Igawa, H. Okada, H. Takahashi, S. Matsuishi, Y. Kamihara, M. Hirano, H. Hosono, K. Matsubayashi, and Y. Uwatoko, *J. Phys. Soc. Jpn.* **78**, 025001 (2009).
- [18] H. Kotegawa, H. Sugawara, and H. Tou, *J. Phys. Soc. Jpn.* **78**, 013709 (2009).
- [19] K. Kitagawa, N. Katayama, H. Gotou, T. Yagi, K. Ohgushi, T. Matsumoto, Y. Uwatoko, and M. Takigawa, *Phys. Rev. Lett.* **103**, 257002 (2009).
- [20] W. O. Uhoya, J. M. Montgomery, G. M. Tsoi, Y. K. Vohra, M. A. McGuire, A. S. Sefat, B. C. Sales, and S. T. Weir, *J. Phys.: Condens. Matter* **23**, 122201 (2011).
- [21] J. J. Wu, J. F. Lin, X. C. Wang, Q. Q. Liu, J. L. Zhu, Y. M. Xiao, P. Chow, and C. Q. Jin, *Sci. Rep.* **4**, 3685 (2014).
- [22] N. V. Morozova, A. E. Karkin, S. V. Ovsyannikov, Y. A. Umerova, V. V. Shchennikov, R. Mittal, and A. Thamizhavel, *Supercond. Sci. Technol.* **28**, 125010 (2015).
- [23] W. Schnelle, A. Leithe-Jasper, R. Gumeniuk, U. Burkhardt, D. Kasinathan, and H. Rosner, *Phys. Rev. B* **79**, 214516 (2009).
- [24] J. S. Kim, S. Khim, H. J. Kim, M. J. Eom, J. M. Law, R. K. Kremer, J. H. Shim, and K. H. Kim, *Phys. Rev. B* **82**, 024510 (2010).
- [25] Y. Muraba, S. Matsuishi, S.-W. Kim, T. Atou, O. Fukunaga, and H. Hosono, *Phys. Rev. B* **82**, 180512(R) (2010).
- [26] F. Weickert, M. Nicklas, W. Schnelle, J. Wosnitza, A. Leithe-Jasper, and H. Rosner, *J. Appl. Phys.* **110**, 123906 (2011).
- [27] M. Gooch, B. Lv, B. Lorenz, A. M. Guloy, and C. W. Chu, *Phys. Rev. B* **78**, 180508(R) (2008).
- [28] K. Ahilan, J. Balasubramanian, F. L. Ning, T. Imai, A. S. Sefat, R. Jin, M. A. McGuire, B. C. Sales, and D. Mandrus, *J. Phys.: Condens. Matter* **20**, 472201 (2008).
- [29] K. Ahilan, F. L. Ning, T. Imai, A. S. Sefat, M. A. McGuire, B. C. Sales, and D. Mandrus, *Phys. Rev. B* **79**, 214520 (2009).
- [30] E. Colombier, M. S. Torikachvili, N. Ni, A. Thaler, S. L. Bud'ko, P. C. Canfield, *Supercond. Sci. Technol.* **23**, 054003 (2010).
- [31] S. Drotziger, P. Schweiss, K. Grube, T. Wolf, P. Adelman, C. Meingast, H. v. Löhneysen, *J. Phys. Soc. Jpn.* **79**, 124705 (2010).
- [32] S. Arsenijević, R. Gaál, A. S. Sefat, M. A. McGuire, B. C. Sales, D. Mandrus, L. Forró, *Phys. Rev. B* **84**, 075148, (2011).
- [33] Y. Zheng, Y. Wang, F. Hardy, A. E. Böhmer, T. Wolf, C. Meingast, and R. Lortz, *Phys. Rev. B* **89**, 054514 (2014).
- [34] Y. Tang, Q. Tao, Z.A. Xu, X.J. Chen, *J. Appl. Phys.* **115**, 143904 (2014).
- [35] M. Nicklas, in: *Strongly Correlated Systems - Experimental Techniques*, edited by A. Avella and F. Mancini (eds.), Springer Series in Solid-State Sciences 180, (Springer, Berlin, Heidelberg, 2015), pp. 173-204.
- [36] T_{SDW} is defined by the position of the inflection point in $\rho(T)$.
- [37] M. S. Torikachvili, S. L. Bud'ko, N. Ni, and P. C. Canfield, *Phys. Rev. Lett.* **101** 057006 (2008).
- [38] M. Nicklas, M. Kumar, E. Lengyel, W. Schnelle and A. Leithe-Jasper, *J. Phys. Conf. Ser.* **273**, 012101 (2011).
- [39] $T_{c,\rho}^{\text{onset}}$, $T_{c,\rho}^{\text{mid}}$, and $T_{c,\rho}^{\text{final}}$ are defined by the temperature where $\rho(T)$ reaches 95%, 50%, and 5% of the normal state resistivity, respectively.
- [40] K.-H. Müller, *Physica C* **159**, 717 (1989).